



Figures and figure supplements

Cortex commands the performance of skilled movement

Jian-Zhong Guo et al

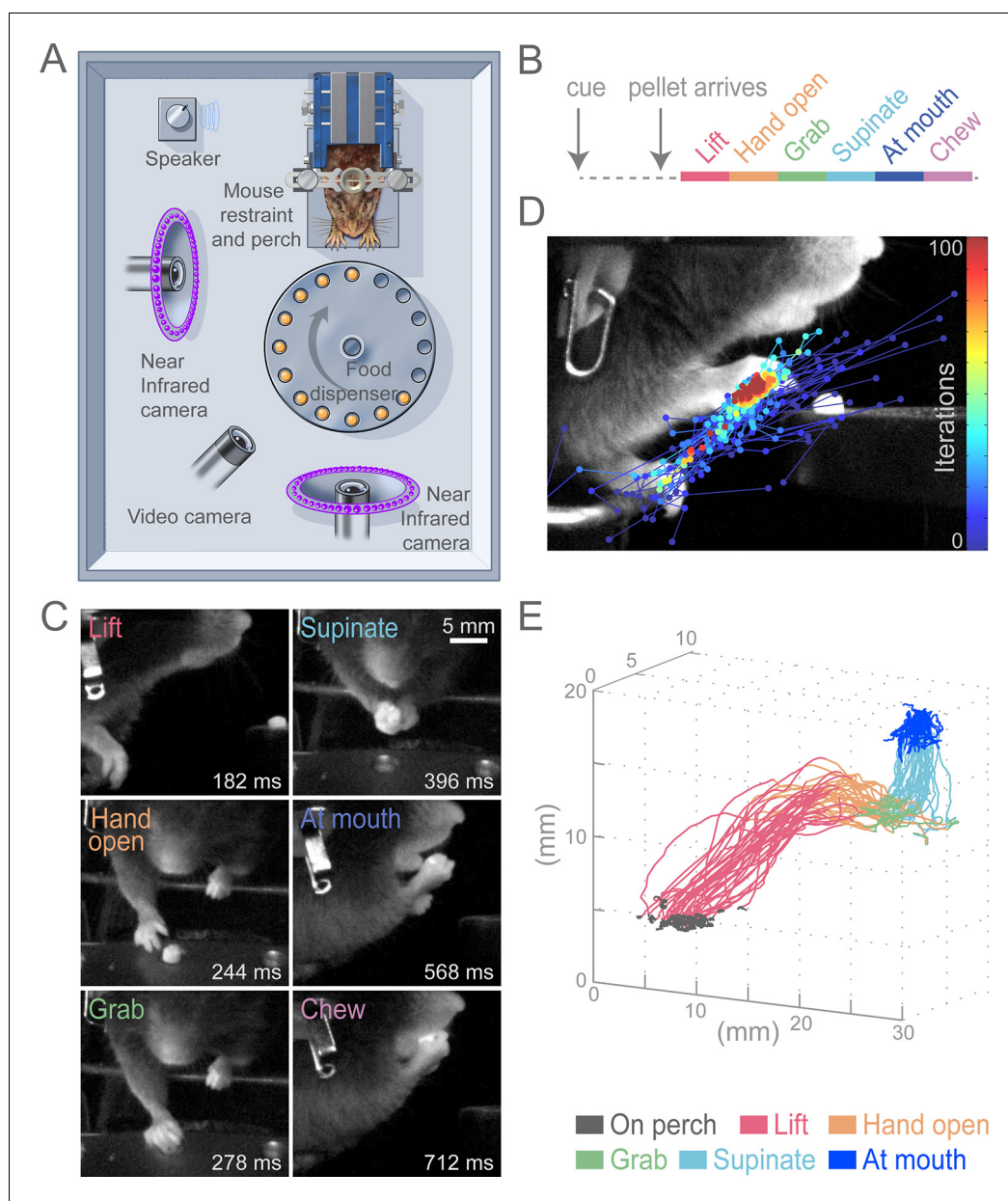


Figure 1. Head-fixed, cued, multi-step, prehension task. (A) Schematic of behavioral arena. Mice reached for and grabbed a food pellet presented on a turntable after an auditory cue. High-speed, near-infrared-sensitive cameras captured video of behavior from perpendicular angles. (B) Timeline of prehension components. Prehension behavior consists of the following elements: lift hand from perch, open hand while reaching, grab pellet, supinate hand, elevate hand to mouth, and chew pellet. (C) Example video frames (front or side views) of each prehension component; times are relative to cue. (D) Visualization of iterations of the Cascaded Pose Regression algorithm used to track the forelimb. Each line corresponds to a random initialization ($n = 50$ initializations) and represents the pose estimates for 100 successive iterations of the tracking algorithm (color indicates iteration). Red dots indicate the distribution of final pose estimates. Our algorithm finds a smooth trajectory over time with high density in this distribution across all frames. (E) Three-dimensional view of stereotyped prehension trajectories (50 trials) of a well-trained animal extracted using the Cascaded Pose Regression algorithm. Behavioral components in the trajectories are color coded as indicated.

DOI: [10.7554/eLife.10774.003](https://doi.org/10.7554/eLife.10774.003)

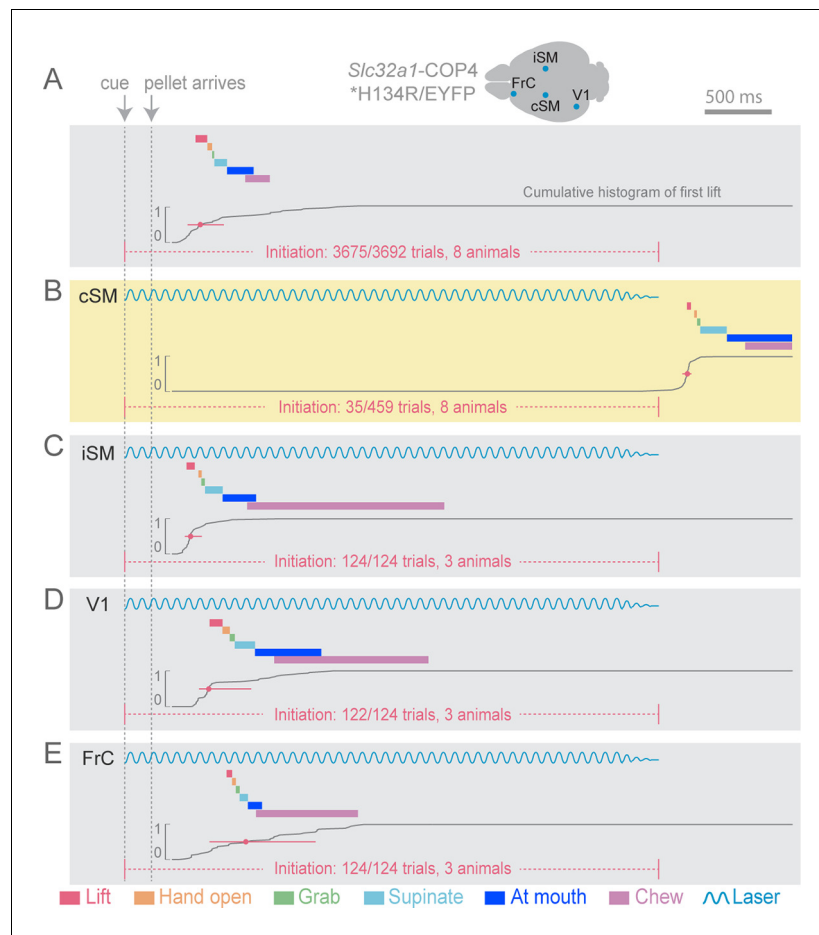


Figure 2. Initiation of head-fixed prehension behavior requires contralateral sensorimotor cortex. Optogenetic stimulation of GABAergic inhibitory neurons in *Slc32a1-COP4**H134R/EYFP mice was used to suppress specific cortical areas, as depicted in the schematic. Laser emission (40 Hz sinusoidal train for 4 s, blue sinusoidal lines) directed through a cleared skull over each cortical area. Depictions of representative ethograms and cumulative histograms for a representative animal. Cumulative histogram is the running total (for all trials) of the occurrence of first list. (A) Tone-cued prehension behavior under control conditions with no optogenetic stimulation. (B–E) Optogenetic inhibition of cortical regions at trial onset. (B) Contralateral sensorimotor cortex (cSM, yellow shading). (C) Ipsilateral sensorimotor cortex (iSM). (D) Visual cortex (V1). (E) Frontal cortex (FrC). Optogenetic inhibition of cSM; but not iSM, V1, or FrC; prevented prehension. Initiation rates over bracketed time period for control and laser trials are listed per condition. Color-coded bars denote behavioral components for (A–E).

DOI: [10.7554/eLife.10774.006](https://doi.org/10.7554/eLife.10774.006)

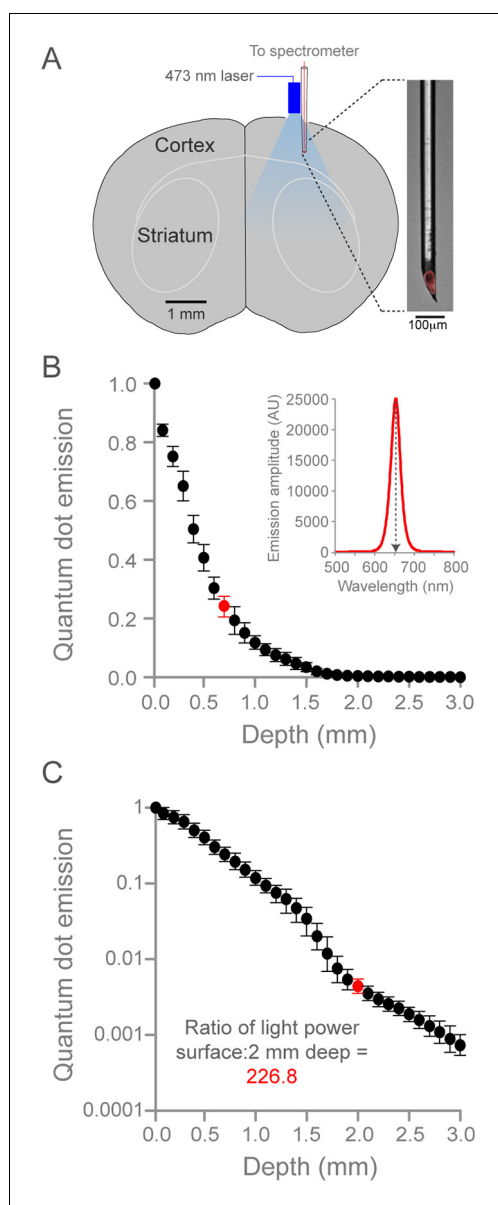


Figure 2—figure supplement 1. Quantification of optogenetic laser intensity at different neural depths. **(A)** Schematic of laser intensity measurements. A custom-made, quantum dot-based photodetector (expanded on right, red is quantum dot fluorescence) and a fiber-coupled 473 nm laser were positioned over a craniotomy above SM cortex. The photodetector was moved at 0.1 mm steps into the brain. **(B)** Relationship between depth from cortical surface and light intensity. Inset, representative spectrogram of quantum-dot fluorescence following 473 nm laser excitation at 0.7 mm below the dural surface (corresponding to red circle in plot, left). Quantum dot emission at 653 nm (normalized arbitrary units) was used to measure intensity of 473 nm light. Data are the mean of three animals, bars are standard deviation. **(C)** Relationship between depth from cortical surface and light intensity

Figure 2—figure supplement 1 continued on next page

Figure 2—figure supplement 1 continued

on log10 scale. Laser intensity decreased more than 225-fold between surface and 2.0 mm deep (red circle, corresponding to the dorsal border of striatum). Note the deviation from exponential laser decay between 1.5 and 2.0 mm depths, potentially caused by densely packed white matter tracks.

DOI: [10.7554/eLife.10774.007](https://doi.org/10.7554/eLife.10774.007)

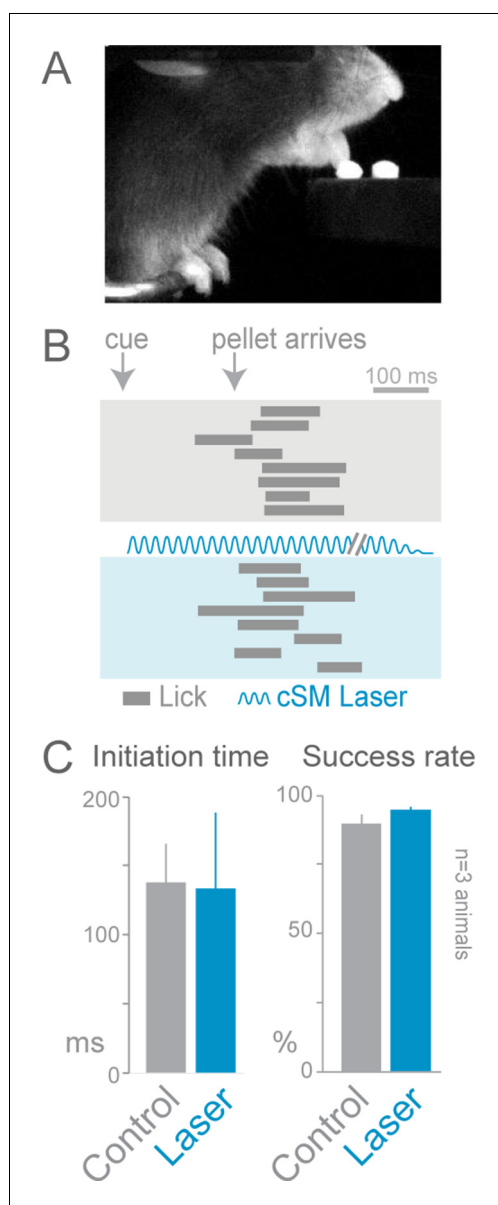


Figure 2—figure supplement 2. Cortical inhibition does not affect cued licking behavior. *Slc32a1*-COP4*H134R/EYFP mice were trained to lick to obtain a food pellet after an auditory cue. (A) Image of animal performing the cued licking task. (B) Ethograms of cued licking (gray bars). Gray box contains control trials, blue box contains laser stimulation trials. Blue sinusoidal line marks laser duration. (C) Comparison of initiation time (left) and success rates (right) for control (gray) and laser-stimulation (blue) trials. Activation of cortical inhibitory neurons (even in cortical areas previously reported to be involved in licking tasks) (Guo et al., 2014) did not disrupt lick initiation or execution ($n = 84$ control trials, $n = 32$ laser trials, t-test with unequal variance, $p > 0.05$). The licking task may not be cortically (unilaterally) dependent because the movement is too simple (one-step task) or the task may

Figure 2—figure supplement 2 continued on next page

Figure 2—figure supplement 2 continued

lack errors that engage the cortex. cSM, contralateral sensorimotor cortex

DOI: [10.7554/eLife.10774.008](https://doi.org/10.7554/eLife.10774.008)

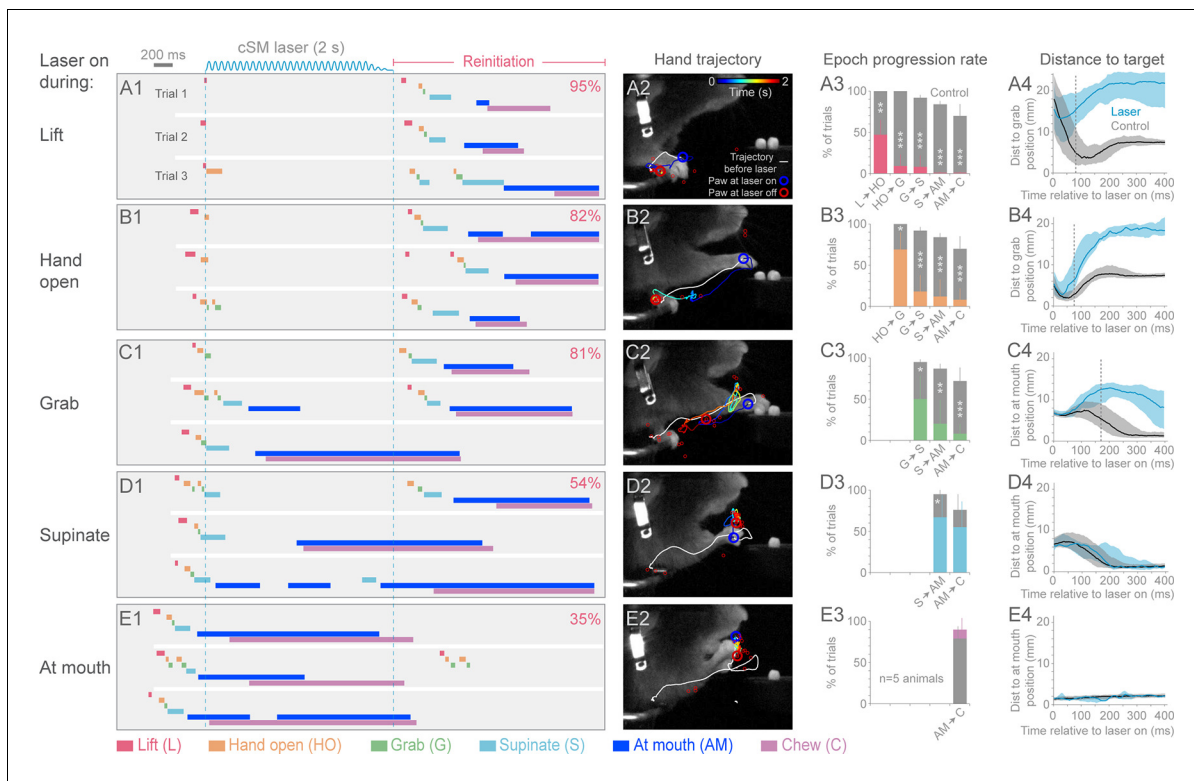


Figure 3. Contralateral sensorimotor cortex is required for the ongoing execution of head-fixed prehension behavior. (A1 to E1) Optogenetic activation of contralateral sensorimotor cortical inhibitory neurons of *Slc32a1-COP4^{H134R}/EYFP* mice during the epochs of tone-cued prehension. Three example trials presented as ethograms for a representative animal. Laser duration marked by sinusoidal and dashed blue lines; behavioral components denoted by color-coded bars (abbreviations indicated). Percentage (top-right, pooled across 5 animals, rate during bracketed time period) of trials where animals reinitiated the behavior upon cessation of cortical inhibition. (A2 to E2) Hand trajectory before and during cortical inhibition of each prehension component. White line labels trajectory from trial start to the onset of inhibition. Colored line represents trajectory during the laser, blue to red color variation represents passing time. Open circles mark hand position at start of inhibition (blue) and end of inhibition (red, small red circles mark laser off position for additional trials). (A3 to E3) Histograms of epoch progression rate, averaged over 5 animals. Control trials are gray and laser trials are the color code of the epoch ongoing at laser onset. For each animal, the number of control trials plotted was equal to the number of laser trials. Control trials were selected based on achievement of at least the epoch ongoing at laser onset. X-axis defines epochs of progression, y-axis represents percent of trials where progression was successful. Progressions where number was not available were removed from the x-axis. Bars are standard deviation. Asterisks indicate statistical significance (t-test with unequal variance, * $p < 0.05$, ** $p < 0.01$, *** $p < 0.001$). (A4 to E4) Path deviations during cortical inhibition of a representative animal. Measurement is the median shortest distance between hand position and either the median Grab or At mouth position. Time is in reference to laser onset. Lines represent control trials (black) and trials with optogenetic cortical inhibition (blue, see Materials and methods). Shaded area surrounding the line represents the 25th and 75th percentiles. Vertical dashed line marks the time when the 25th and 75th percentiles no longer overlap.

DOI: 10.7554/eLife.10774.023

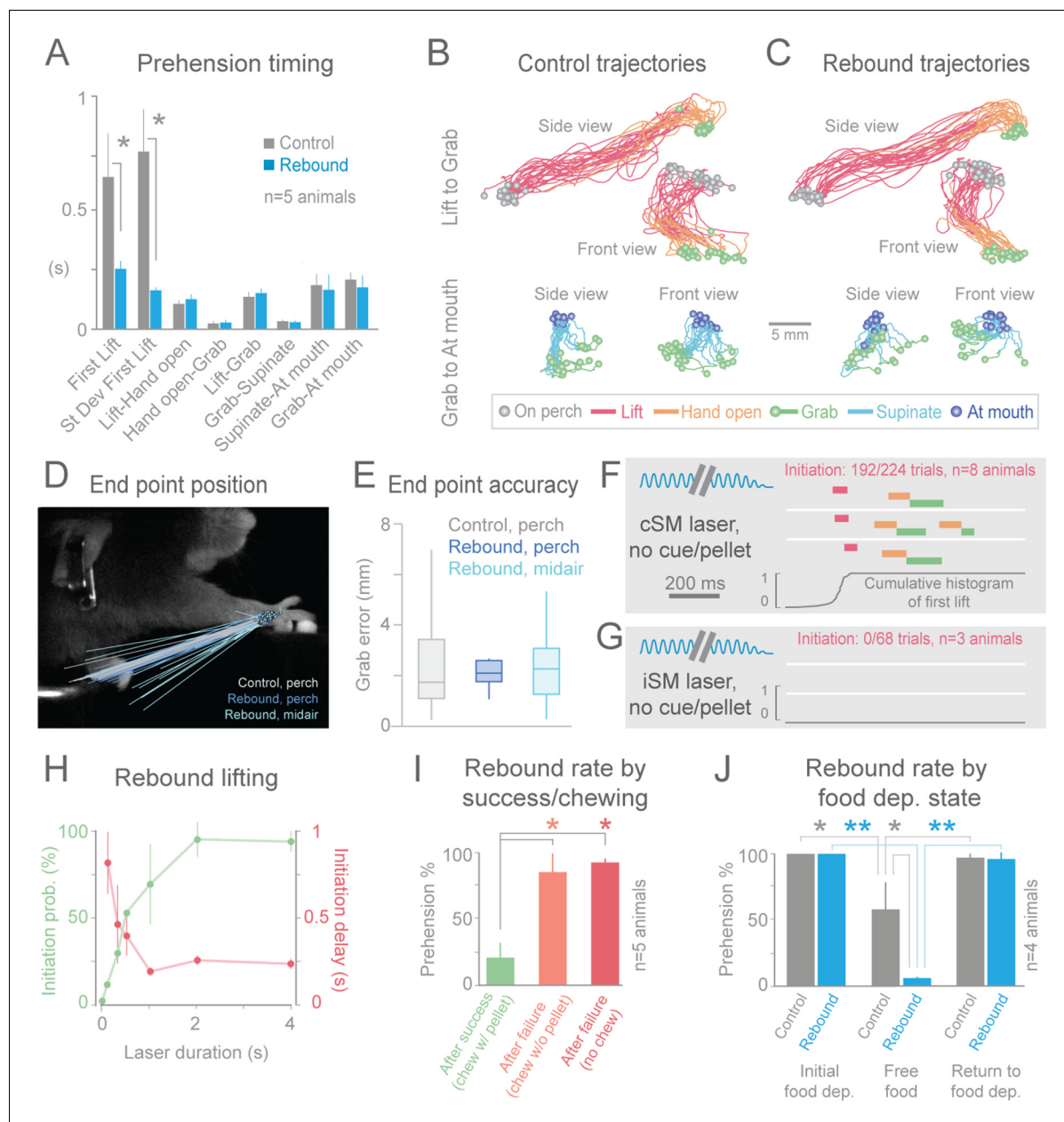


Figure 4. Termination of cortical inhibition is sufficient to generate normal prehension behavior. (A) Timing differences between control prehension behavior and prehension after laser termination ("rebound prehension"), averaged across 5 *Slc32a1*-COP4*H134R/EYFP animals. Values include First Lift (difference between First Lift and either the cue (control) or laser off (rebound)) and the intervals between sequential behavioral components. Within individual animals, First Lift timing (3/5 animals) and variance (5/5 animals) were also significantly different (Wilcoxon–Mann–Whitney rank sum, $p < 0.05$). (B and C) Comparison of the trajectories of control (B) and rebound prehension (C) Trajectories (n = 20 trials) color coded by behavioral component. Top row displays trajectories from Lift to Grab, bottom row represents trajectories from Grab to At mouth. Circles represent on perch (gray), Grab (green), and At mouth (dark blue) hand position. (D) Rebound prehension was accurately performed from a diversity of starting positions. Control prehension from the perch (gray, n = 25 trials), rebound prehension from perch (dark blue, n = 25 trials), and rebound prehension from mid-air starting position (light blue, n = 18 trials) for a representative animal. Lines connect starting position of the reach to Grab position. Color-coded circles represent Grab position. (E) End-point quantification for control, rebound prehension from perch, and rebound prehension from mid-air trials for a representative animal. Box plots (whiskers mark minimum and maximum non-outliers) of Grab error: Grab error is defined as the distance between Grab position of an individual trial and median Grab position (control, success trials). No significant difference between control and rebound prehension from the perch or from midair positions (4/5 and 5/5 animals, respectively; Wilcoxon–Mann–Whitney rank sum, $p > 0.05$). (F) Extinguishing the laser over contralateral sensorimotor cortex elicited rebound prehension even in the absence of a cue and pellet. (G) Laser-off over ipsilateral sensorimotor cortex did not generate rebound prehension. (F) and (G) Behavioral components denoted by color-coded bars. Blue sinusoidal line marks

Figure 4 continued on next page

Figure 4 continued

laser duration. Cumulative histogram of First Lift is shown. (H) Effect of laser duration on the likelihood of rebound prehension, initiation latency, and associated jitter in the absence of cue and pellet. Statistically significant (repeated-measures ANOVA, $p < 0.05$) main effect of laser duration on rebound prehension initiation probability, delay, and jitter. (I) Rate of rebound prehension as a function of success and chewing status at laser off (average of 5 animals, bars are standard deviation). (J) Control (gray) and rebound (blue) prehension rates as a function of food deprivation (dep.) state. Animals ($n = 4$) were taken off food deprivation three times and the rates were averaged. Prehension rates plotted are the means of these averages, bars are standard deviation. Asterisks indicate statistical significance (t-test with unequal variance, $*p < 0.05$, $**p < 0.001$).

DOI: [10.7554/eLife.10774.024](https://doi.org/10.7554/eLife.10774.024)

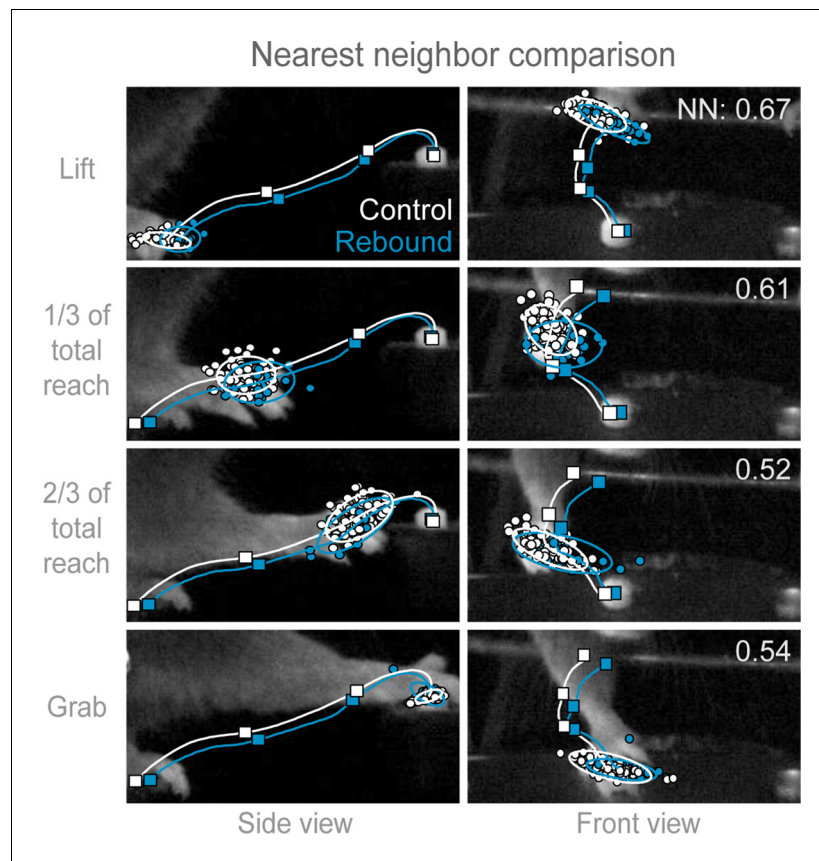


Figure 4—figure supplement 1. Trajectories of control and rebound prehension are similar. Comparison of the average trajectory of control (white line) and rebound (blue line) prehension of *Slc32a1-COP4*H134R/EYFP* mice. Squares on line mark average hand position at Lift, 1/3 of total reach, 2/3 of total reach, and Grab position. Side (left column) and front (right column) views of head-fixed mouse. Rows display clouds of hand position (filled-circles) for Lift, 1/3 of total reach, 2/3 of total reach, and Grab position. Open circles marks 2-sigma ellipse describing the sample mean and covariance of hand position. Number in upper right corner indicates the balanced nearest neighbor (NN) accuracy (score of 0.5 reflects chance assignment to control or rebound prehension groups, see Materials and methods).

DOI: [10.7554/eLife.10774.025](https://doi.org/10.7554/eLife.10774.025)

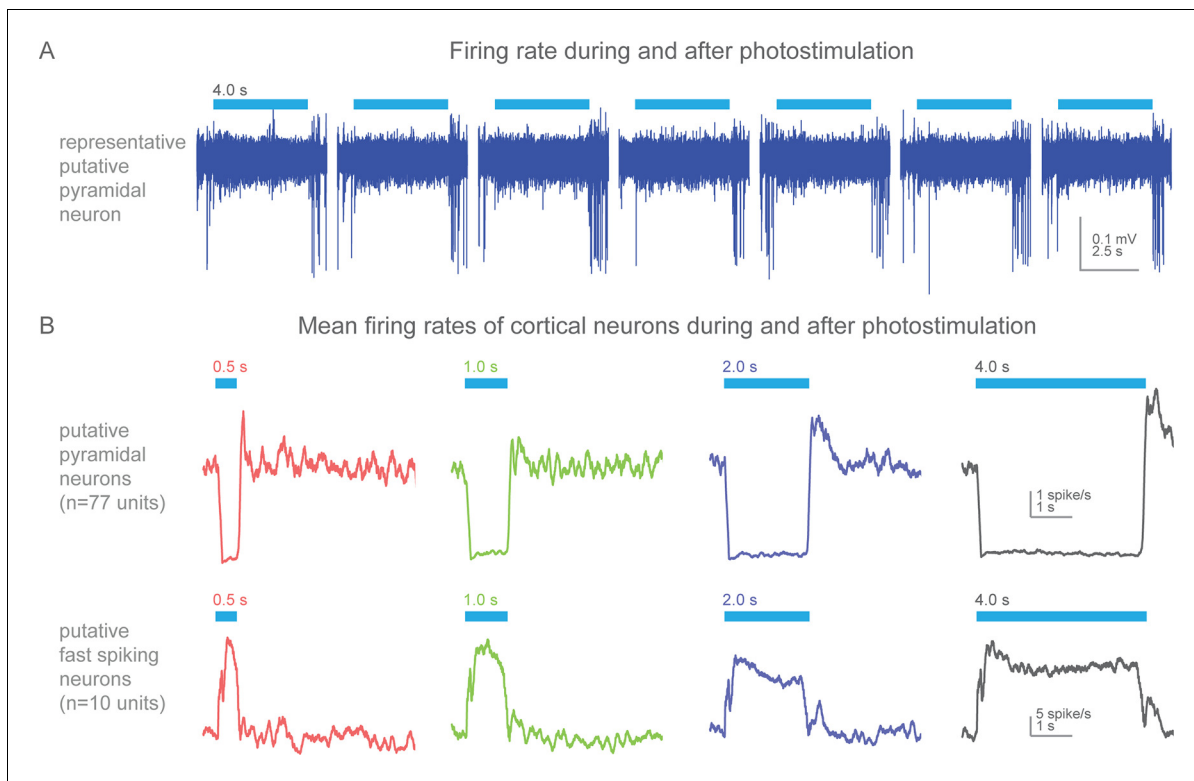


Figure 4—figure supplement 2. Action potential firing rates during and after photostimulation in cortical neurons of awake, non-behaving *Slc32a1-COP4*H134R/EYFP* mice. **(A)** Silicon probe extracellular recordings of a putative pyramidal cortical neuron. Blue line represents 4 s of 473 nm light (7 mW). Increased spiking immediately at the termination of each light exposure. **(B)** Mean firing rates (peristimulus time histograms, 100 ms bins) for putative pyramidal (spike width >0.45 ms) and fast spiking (spike width <0.35 ms) cortical neurons around photostimulation. Columns, four different durations of photostimulation (blue bars). Top row, mean of putative pyramidal neurons (n = 77 units, 2 mice). Bottom row, mean of putative fast spiking neurons (n = 10 units, 2 mice). Prominent rebound activity is seen with light exposure of 2 s and greater.

DOI: [10.7554/eLife.10774.026](https://doi.org/10.7554/eLife.10774.026)

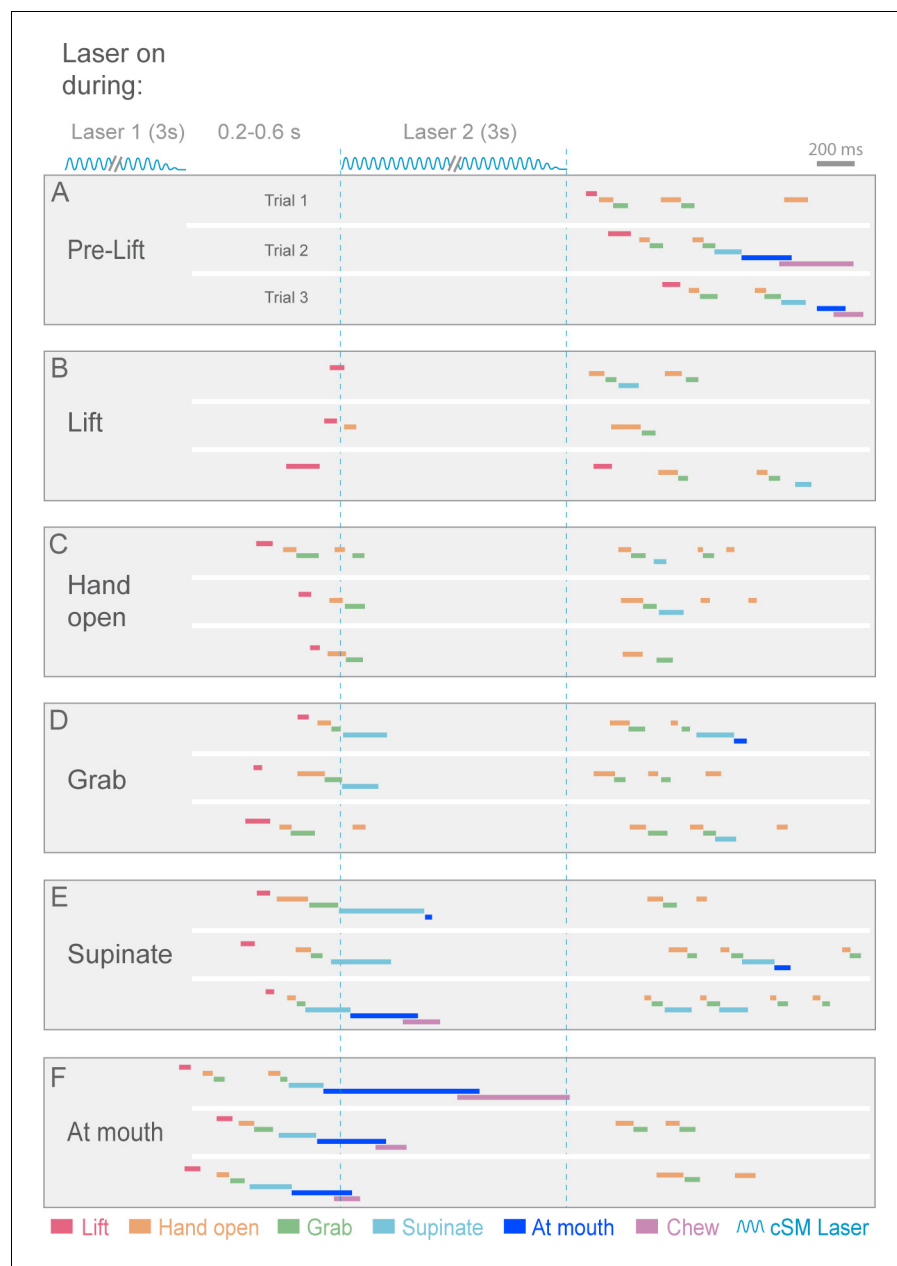


Figure 4—figure supplement 3. Contralateral sensorimotor cortex is required for the ongoing execution of rebound prehension. (A–F) Termination of initial optogenetic activation (laser 1) of sensorimotor cortical inhibitory neurons of *Slc32a1-COP4^{H134R}/EYFP* mice elicited rebound prehension; second laser (laser 2) administration interrupts rebound prehension. Examples of laser exposure during each component of rebound prehension are shown. Laser duration is marked by sinusoidal and dashed blue lines and behavioral components are denoted by color-coded bars. Similar to control prehension, cortical inhibition froze progression of rebound prehension. Termination of second laser exposure elicited another rebound prehension.

DOI: [10.7554/eLife.10774.027](https://doi.org/10.7554/eLife.10774.027)